Hall Coefficient for the Two-Dimensional Hubbard Model

F. F. Assaad and M. Imada
Institute for Solid State Physics, University of Tokyo, 7-22-1 Roppongi, Minato-ku, Tokyo 106, Japan
(Received 8 December 1994)

We calculate with quantum Monte Carlo methods the Hall coefficient R_H for the 2D Hubbard model at small hole doping near half filling. In the weak coupling regime R_H is electronlike. In the strong coupling regime, where the mapping to the t-J model is justified, R_H is electronlike with small amplitude in the temperature regime $T > U$, $T < J$ and holelike in the temperature regime $J < T < U$. Our results are consistent with the picture of a Mott transition driven by the divergence of the effective mass as opposed to the vanishing of the number of charge carriers.

PACS numbers: 71.27.+a, 71.30.+h

In the Drude description of metals, the Drude weight is given by $D = \pi e^2 n/m$ and the Hall coefficient by $R_H = 1/nec$ where n (m) denotes the density (effective mass) of charge carriers in the relevant single-particle description. As pointed out by one of the authors [1,2], those equations imply that a continuous metal-insulator transition as a function of doping, and characterized by the vanishing of the Drude weight, may be caused either by the divergence of the effective mass or by the vanishing of the number of charge carriers. In the latter case, the above picture implies that R_H diverges at the transition. In the former case, no singularity in R_H is expected at the transition. Hall experiments on high-T_c compounds at low temperatures are consistent with the picture of a Mott transition driven by the vanishing of the number of charge carriers: a holelike Hall coefficient which shows an unbounded increase in amplitude as the hole doping is decreased [3]. As the temperature is increased, experiments show a remarkable reduction of R_H to values consistent with a carrier number satisfying the Luttinger volume [4,5]. The low temperature properties stand in contradiction with band-structure predictions of the Fermi surface [6], thus pointing out the importance of correlation effects. The purpose of this Letter is to present exact (within statistical error) numerical results for the Hall coefficient at finite and infinite Matsubara frequencies on small clusters for the weak and strong coupling Hubbard models. Based on those calculations, we argue that the *low* temperature Hall coefficient for the hole-doped Hubbard model is electronlike and hence does not show a singular behavior in the vicinity of the Mott transition. This conclusion is valid in both the weak and strong coupling regimes.

Our starting point is the two-dimensional Hubbard model in a transverse magnetic field,

$$H = \sum_{\langle \vec{i},\vec{j}\rangle,\sigma} t_{\vec{i},\vec{j}}\left(\vec{A}\right) c^{\dagger}_{\vec{i},\sigma} c_{\vec{j},\sigma} + U \sum_{\vec{i}} n_{\vec{i},\uparrow} n_{\vec{i},\downarrow} . \qquad (1)$$

Here, $\langle \vec{i},\vec{j}\rangle$ denotes nearest neighbors, $c^{\dagger}_{\vec{i},\sigma}$ ($c_{\vec{i},\sigma}$) creates (annihilates) an electron with a z component of spin σ on site $\vec{i}$ and $n_{\vec{i},\sigma} = c^{\dagger}_{\vec{i},\sigma} c_{\vec{i}\sigma}$. The hopping matrix elements contain the Peierls phase factors, $t_{\vec{i},\vec{j}}(\vec{A}) = -t \exp[(2\pi i/\Phi_0) \int_{\vec{i}}^{\vec{j}} \vec{A} \cdot d\vec{l}\,]$, where Φ_0 is the flux quantum and in the Landau gauge $\vec{A}(\vec{x}) = -B(y,0,0)$. The square lattice lies in the $\vec{e}_x$,$\vec{e}_y$ plane. To reduce finite size effects we consider a torus geometry. Hence the smallest magnetic field one may consider is given by $Ba^2/\Phi_0 = 1/L^2$, where a is the lattice constant and L is the linear number of sites [7]. Because of the above constraint, the extrapolation to small magnetic fields is coupled to the thermodynamic limit.

The linear response to a time dependent electric field $\vec{E}(t) = \vec{E}(\omega)\exp(-i\omega t)$ yields the conductivity tensor $\sigma_{\alpha,\gamma}(i\omega_m) = (e^2/\hbar\omega_m) D_{\alpha,\gamma}(i\omega_m)$, where

$$D_{\alpha,\gamma}(i\omega_m) = \frac{1}{L^2}\left(-\frac{\langle K\rangle}{2}\,\delta_{\alpha,\gamma} - \int_0^{\beta} d\tau\, e^{i\omega_m \tau} \langle\, j_\alpha(\tau) j_\gamma(0)\rangle\right). \qquad (2)$$

In the above equation, $\omega_m = 2\pi m/\beta$ are Matsubara frequencies, β is the inverse temperature, $\langle K\rangle$ denotes the thermal average of the kinetic energy in Eq. (1), and $j_\alpha = -i \sum_{\vec{i},\sigma} [t_{\vec{i},\vec{i}+\vec{a}_\alpha}(\vec{A})\, c^{\dagger}_{\vec{i},\sigma} c_{\vec{i}+\vec{a}_\alpha,\sigma} - t_{\vec{i}+\vec{a}_\alpha,\vec{i}}(\vec{A})\, c^{\dagger}_{\vec{i}+\vec{a}_\alpha,\sigma} c_{\vec{i},\sigma}]$. We define R_H by

$$R_H(B, i\omega_m) = \frac{1}{B}\,\frac{\sigma_{x,y}(i\omega_m)}{\sigma^2_{x,x}(i\omega_m) + \sigma^2_{x,y}(i\omega_m)} . \qquad (3)$$

At zero temperature, one may show that $\lim_{i\omega_m \to 0} \lim_{B\to 0} R_H(B, i\omega_m) = \lim_{\omega\to 0} \lim_{B\to 0} R_H(B,\omega)$ [10]. Hence the static, zero temperature Hall coefficient may be obtained by extrapolating to zero Matsubara frequency. The high frequency Hall coefficient ($\omega_m \gg U, t$) [8] is given by

$$R^{\star}_H = R_H(B, \omega \to \infty) = R_H(B, i\omega_m \to i\infty) = -\frac{4\hbar L^2}{e^2 B}\,\frac{i\langle(\, j_x, j_y)\rangle}{\langle K\rangle^2} . \qquad (4)$$

The experimental relevance of $R^{\star}_H$ is discussed in [8].

Figure 1 plots $R_H(B, i\omega_m)$ for free electrons [i.e., $U/t = 0$ in Eq. (1)] at essentially zero temperature ($\beta t \equiv t/T = 10^4$) and band filling $\langle n\rangle = 0.80$. The finite

 0031-9007/95/74(19)/3868(4)$06.00 © 1995 The American Physical Society

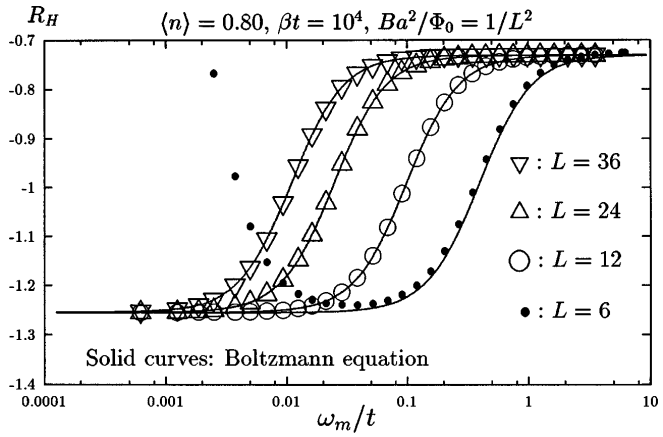

FIG. 1. $R_H(B, i\omega_m)$ in units of $a^2/|e|c$ for free electrons. Solid curves show solutions of the Boltzmann equation (see text).

lattice results (symbols) are compared to the prediction of the Boltzmann transport equation in the relaxation time approximation (solid curves) [9,10]. As appropriate for free electrons, we set the relaxation time $\tau = \infty$. There are no fitting parameters and the magnetic field is scaled as $Ba^2/\Phi_0 = 1/L^2$. Several points may be made. (i) Perfect agreement with the Boltzmann equation is obtained except for the low frequency data for the 6×6 lattice where the discrepancy is due to energy gaps in finite size systems. (ii) The crossover between the high and low frequency values of R_H occurs at the cyclotron frequency ω_H. Note that in the special case of a circular Fermi surface, R_H is frequency independent. The low frequency value of R_H converges to the Drude result, $-a^2/(\langle n\rangle |e|c)$. The high frequency value of R_H (4) converges to the prediction of the Boltzmann equation in the weak field limit (i.e., $\omega_H \tau \ll 1$). This may be understood by noting that if the frequency of the applied electric field is much larger than ω_H, the semiclassical motion of the electron on the Fermi surface will be perturbed before accomplishing a full revolution. The same picture applies in the weak field limit. As shown by this simple example, and as argued by Shastry, Shraiman, and Singh [8], R_H in the high frequency limit is related to the semiclassical Hall coefficient. (iii) $\lim_{i\omega_m \to 0} \lim_{B \to 0} R_H(B, i\omega_m)$ scales to the static Hall coefficient as obtained from the Boltzmann transport equation in the weak field limit.

We calculate the conductivity tensor along the imaginary time axis for the Hubbard model with finite temperature quantum Monte Carlo (QMC) methods [11]. The generalization of QMC algorithms to incorporate magnetic fields has been discussed in Ref. [12]. In order to reduce fluctuations in the QMC calculation of D_{xy}, we have included an infinitesimal *electric field* (i.e., imaginary time dependent vector potential) in the imaginary time propagation. The conductivity tensor is then obtained by numerical differentiation with respect to the *electric field*. The details of this approach will be described elsewhere [10].

Figure 2 plots $R_H(B, i\omega_m)$ for the weak coupling Hubbard model ($U/t = 4$) on 6×6 lattices and at $\beta t = 5$ [13]. Similar results were obtained on 4×4 lattices. One may see that the QMC results compare well with the $U/t = 0$ value of R_H (solid lines) for all considered band fillings. At the considered temperature, R_H shows no singular behavior as the Mott transition is approached (i.e., $\langle n\rangle \to 1$). This stands in agreement with the QMC calculation of the charge susceptibility by Furukawa and Imada [14] which supports the picture of a Mott transition driven by the divergence of the effective mass.

We now consider the strong coupling Hubbard model $U/t > 8$, where the mapping onto the t-J model with $J = 4t^2/U$ is valid. Figure 3(a) plots $R_H^\star$ for several choices of U/t and as a function of temperature. We consider the filling $\langle n\rangle = 0.95$. Although we cannot reach temperatures $T \ll J$ due to the sign problem, the general features of the data show that there is an intermediate temperature regime where $R_H^\star$ is positive (holelike). At high and low temperatures, $R_H^\star$ is negative (electronlike). We may classify the data by considering three temperature regimes. (i) $T > U$. Here, correlation effects may, to a first approximation, be neglected: $R_H^\star$ is negative and scales to its free electron value. (ii) $J < T < U$. In this temperature regime, the energy scale J is hidden by thermal fluctuations. This may be confirmed by considering antiferromagnetic spin-spin correlations $S(\pi, \pi) = \frac{4}{3} \sum_j \exp(i\vec{Q}\vec{j}\,)\langle \vec{S}(\vec{j}\,) \cdot \vec{S}(\vec{0}\,)\rangle$, where $\vec{Q} = (\pi, \pi)/a$ and $\vec{S}(\vec{j}\,)$ is the spin operator on site $\vec{j}$. As may be seen from Fig. 3(b) $S(\pi, \pi)$ takes values independent of $J = 4t^2/U$ in the considered temperature regime. Hence, for $J < T < U$, the physics of the Hubbard model is related to that of the $U = \infty$ Hubbard model. We can make contact with the work of Shastry, Shraiman, and Singh [8] who have calculated $R_H^\star$ for the t-J model only in the region $T > J$ by a high temperature expansion. Before comparing results, we note that Shastry, Shraiman,

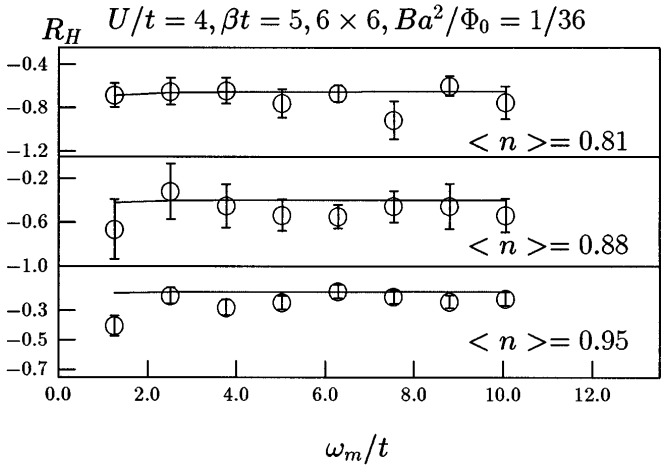

FIG. 2. $R_H(B, i\omega_m)$ in units of $a^2/|e|c$ for the weak coupling Hubbard model (open circles). Solid lines correspond to the $U/t = 0$ values of $R_H(B, i\omega_m)$.

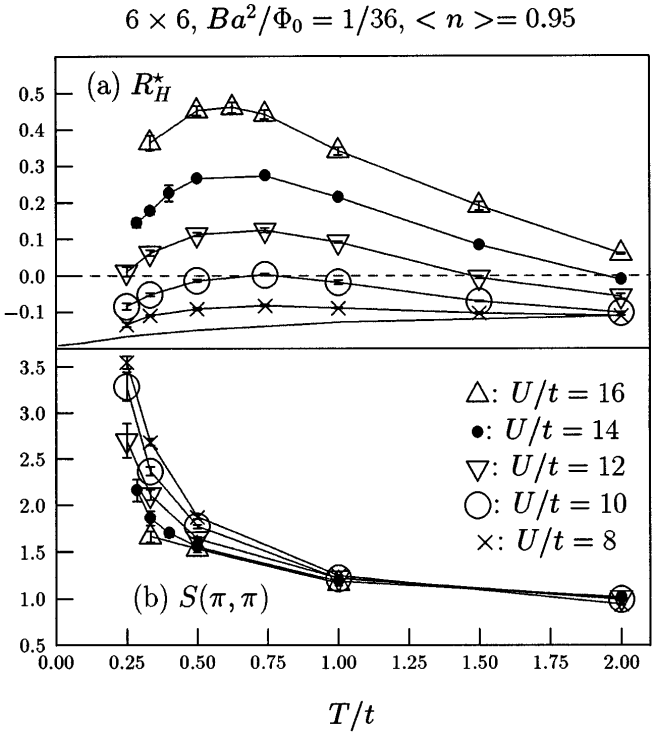

FIG. 3. (a) $R_H^\star$ as a function of temperature for the strong coupling Hubbard model. Solid line with no symbols corresponds to the $U/t = 0$ value of $R_H^\star$. (b) Antiferromagnetic spin-spin correlations for the Hubbard model as a function of temperature.

and Singh [8] perform their calculations within the projected Hilbert space of no double occupancy. Hence Eq. (4) corresponds to frequencies $\omega \gg J$, but $\omega \ll U$. Figure 3(a) shows a holelike $R_H^\star$ for $J < T < U$. One also notes that $R_H^\star$ decreases as $T \to J$. These results are consistent with Ref. [8]. (iii) $T < J$. The energy scale J may be singled out by considering the antiferromagnetic spin-spin correlations [Fig. 3(b)]. As apparent from Figs. 3(a) and 3(b), the reduction of $R_H^\star$ is directly related to the enhancement of $S(\pi,\pi)$ at $T \lesssim J$. A natural extrapolation of the results in Fig. 3 yields an electronlike $R_H^\star$ in the considered temperature regime.

The density dependence of $R_H^\star$ is given in Fig. 4 at $U/t = 12$, $\beta t = 1.35$ ($J < T < U$), and $\beta t = 3.5$ ($T < J$). At those temperatures, no finite size effects are observed. Since we have not projected out the upper-Hubbard band, particle-hole symmetry present at half band filling leads to the vanishing of the Hall coefficient at any frequency. At small densities, $R_H^\star$ scales to it's free electron value. The maximal value of $R_H^\star$ is approximately located at $\langle n \rangle = 0.95$ which is the density considered in Fig. 3. As the temperature is lowered, the density interval for which $R_H^\star$ is holelike as well as the magnitude of $R_H^\star$ diminishes. At lower temperatures, we expect $R_H^\star$ to be negative (electronlike) at any hole doping in this model. This is confirmed by the data in Fig. 4 for a 4×4 lattice at $\beta t = 5$. Apart from the vanishing of

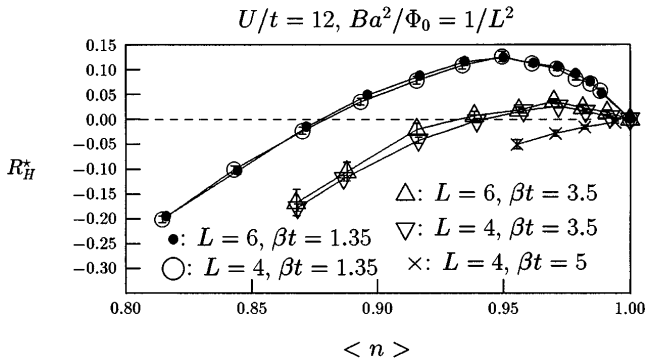

FIG. 4. Density dependence of $R_H^\star$ for the strong coupling Hubbard model.

$R_H^\star$ at half band filling due to particle-hole symmetry, the data in the temperature regime $J < T < U$ show the same overall structure as observed in Ref. [8].

We have up till now considered frequencies $\omega_m \gg U, t$. Figure 5 (in which Ref. [15] is cited) plots R_H as well as D_{xx} in Eq. (4) at finite Matsubara frequencies for several choices of U/t and temperatures. Upon analysis of low temperature data [Figs. 5(a)–5(d)], one may see that no finite size effects are observable within the obtained accuracy. Since the magnetic field is scaled as $Ba^2/\Phi_0 = 1/L^2$, no spurious effects due to too large values of B are present in Fig. 5. Several points may be made. (i) Extrapolating $D_{xx}(i\omega_m)$ to zero frequency yields $D\hbar^2/\pi e^2$, where D is the Drude weight [16]. A straightforward extrapolation of the data in Fig. 5(a) yields a Drude weight in agreement with independent calculations of Dagotto *et al.* [15]. (ii) In the temperature regime $T < J$, Fig. 5(b), R_H is negative for all considered Matsubara frequencies. R_H decreases with decreasing ω_m but retains small amplitude comparable to $a^2/\langle n \rangle |e| c$. A similar behavior is seen at a slightly higher temperature [Fig. 5(c)]. (iii) In contrast, in the temperature regime $J < T < U$, R_H is positive and increases considerably with decreasing Matsubara frequencies [$U/t = 16$, $T/t = 1$ in Fig. 5(e)]. It is interesting to consider the data for $U/t = 12$. At $T/t = 1$ [Fig. 5(e)] R_H is positive. As the temperature is lowered to $T/t = 1/2$ [Fig. 5(d)], one may see an explicit sign change in R_H at small Matsubara frequencies. From Fig. 5, one may conclude that at lower Matsubara frequencies the overall temperature dependence of the sign of R_H is similar to $R_H^\star$. However, the quantitative magnitude of R_H is frequency dependent.

Our results at $T < J$ are consistent with R_H in the cuprates at higher temperatures, where R_H is insensitive to the doping concentration and has small amplitude [4]. At the moment, we have not obtained any crossover observed in the cuprates. The mechanism of this crossover should be further explored [2].

In summary, we have presented numerical results which strongly support that the Hall coefficient for the weak coupling Hubbard model is electronlike with small

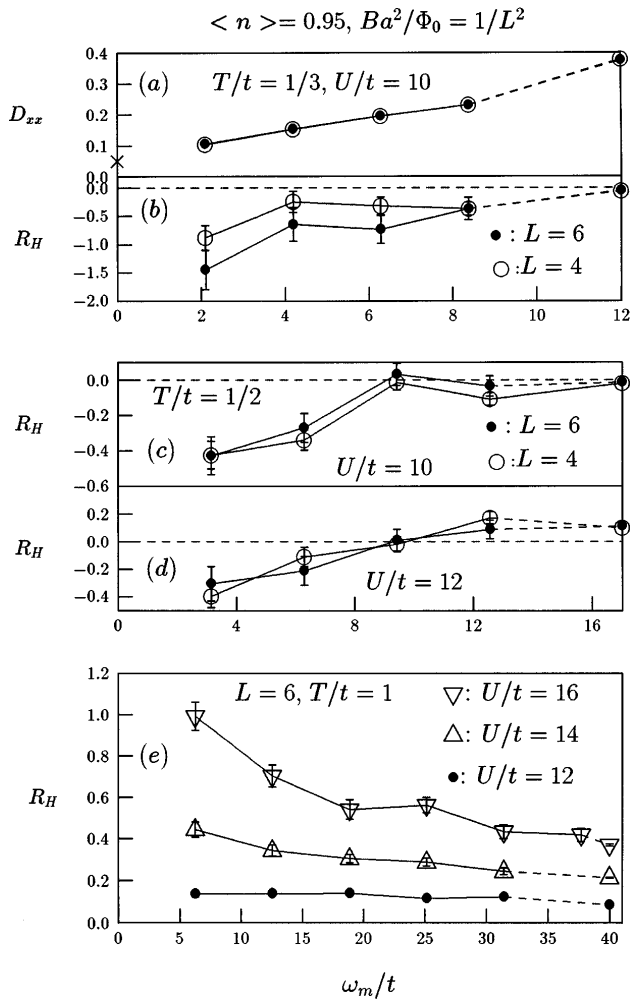

FIG. 5. (a) D_{xx} in units of t. The cross at $i\omega_m = 0$ corresponds to $D\hbar^2/\pi e^2$ as obtained from Ref. [15]. (b)–(e) $R_H(B, i\omega_m)$ in units of $a^2/|e|c$.

amplitude at small hole doping. In the strong coupling regime, where the Hubbard model may be approximately mapped onto the t-J model, the sign of the Hall coefficient was found to be strongly temperature dependent at small hole doping, holelike for $J < T < U$, electronlike with small amplitude for $T < J$ and $T > U$. The overall features of those results were found to be valid at infinite and finite Matsubara frequencies, thus lending support that the static Hall coefficient shows a similar temperature behavior. We note that a similar behavior of the static Hall coefficient was recently obtained by Jarrell [17] from QMC simulations of the $D = \infty$ Hubbard model in the strong coupling regime. Our results are consistent with the high temperature expansion of Shastry, Shraiman, and Singh [8] for the t-J model at $i\omega_m \to \infty$ and in the temperature region $J < T < U$. We have, furthermore, been able to reach lower temperatures, $T < J = 4t^2/U$ for values of $U/t > 8$, and found R_H to change from holelike to electronlike as the temperature scale J is crossed. Finally, our conclusions are in agreement with the picture of a Mott transition driven by the divergence of the effective mass as opposed to the vanishing of the density of charge carriers.

This work is financially supported by a Grant-In-Aid for Scientific Research on Priority Areas from the Ministry of Education Science and Culture of Japan.

[1] M. Imada, J. Phys. Soc. Jpn. **62**, 1105, (1993).
[2] M. Imada, J. Phys. Soc. Jpn. **63**, 3059 (1994).
[3] N. P. Ong *et al.,* Phys. Rev. B **35**, 8807 (1987); H. Takagi *et al., ibid.* **40**, 2254 (1989).
[4] T. Nishikawa, J. Takeda, and M. Sato, J. Phys. Soc. Jpn. **62**, 2568 (1993).
[5] H. Y. Hwang *et al.,* Phys. Rev. Lett. **72**, 2636 (1994).
[6] W. E. Pickett, Rev. Mod. Phys. **61**, 433 (1989).
[7] E. Fradkin, *Field Theories of Condensed Matter Systems* (Addison-Wesley, Reading, 1991), Chap. 9, p. 256.
[8] B. S. Shastry, B. I. Shraiman, and R. P. Singh, Phys. Rev. Lett. **70**, 2004 (1993).
[9] J. M. Ziman, *Electrons and Phonons* (Clarendon, Oxford, 1960), Sec. 12.
[10] F. F. Assaad and M. Imada (unpublished).
[11] J. E. Hirsch, Phys. Rev. B **31**, 4403 (1985); S. R. White, D. J. Scalapino, R. L. Sugar, E. Y. Loh, J. E. Gubernatis, and R. T. Scalettar, *ibid.* **40**, 506 (1989).
[12] F. F. Assaad, W. Hanke, and D. J. Scalapino, Phys. Rev. B **50**, 12 835 (1994).
[13] We have checked that presence of the magnetic field does not affect in a significant way the magnitude of the Hubbard gap and antiferromagnetic spin-spin correlations at half band filling and $U/t = 4$.
[14] N. Furukawa and M. Imada, J. Phys. Soc. Jpn. **62**, 2557 (1993).
[15] E. Dagotto, A. Moreo, F. Ortilani, D. Poilblanc, and J. Riera, Phys. Rev. B **45**, 10 741 (1992).
[16] D. J. Scalapino, S. R. White, and S. C. Zhang, Phys. Rev. Lett. **68**, 2830 (1992); Phys. Rev. B **47**, 7995 (1993).
[17] M. Jarrell (private communication).